

# Altered white matter microarchitecture in Parkinson's disease: a voxel-based meta-analysis of diffusion tensor imaging studies

Xueling Suo<sup>1</sup>, Du Lei (✉)<sup>1,2</sup>, Wenbin Li<sup>1,2</sup>, Lei Li<sup>1</sup>, Jing Dai<sup>3</sup>, Song Wang<sup>1</sup>, Nannan Li<sup>4</sup>, Lan Cheng<sup>4</sup>, Rong Peng<sup>4</sup>, Graham J Kemp<sup>5</sup>, Qiyong Gong (✉)<sup>1,6</sup>

<sup>1</sup>Huaxi MR Research Center (HMRRRC), Department of Radiology, West China Hospital of Sichuan University, Chengdu 610041, China; <sup>2</sup>Department of Psychiatry and Behavioral Neuroscience, University of Cincinnati, Cincinnati, Ohio, USA; <sup>3</sup>Department of Psychoradiology, Chengdu Mental Health Center, Chengdu 610041, China; <sup>4</sup>Department of Neurology, West China Hospital of Sichuan University, Chengdu 610041, China; <sup>5</sup>Liverpool Magnetic Resonance Imaging Centre (LiMRIC) and Institute of Ageing and Chronic Disease, University of Liverpool, Liverpool L69 3GE, United Kingdom; <sup>6</sup>Psychoradiology Research Unit of Chinese Academy of Medical Sciences, West China Hospital of Sichuan University, Chengdu 610041, China

© Higher Education Press 2020

**Abstract** This study aimed to define the most consistent white matter microarchitecture pattern in Parkinson's disease (PD) reflected by fractional anisotropy (FA), addressing clinical profiles and methodology-related heterogeneity. Web-based publication databases were searched to conduct a meta-analysis of whole-brain diffusion tensor imaging studies comparing PD with healthy controls (HC) using the anisotropic effect size–signed differential mapping. A total of 808 patients with PD and 760 HC coming from 27 databases were finally included. Subgroup analyses were conducted considering heterogeneity with respect to medication status, disease stage, analysis methods, and the number of diffusion directions in acquisition. Compared with HC, patients with PD had decreased FA in the left middle cerebellar peduncle, corpus callosum (CC), left inferior fronto-occipital fasciculus, and right inferior longitudinal fasciculus. Most of the main results remained unchanged in subgroup meta-analyses of medicated patients, early stage patients, voxel-based analysis, and acquisition with <30 diffusion directions. The subgroup meta-analysis of medication-free patients showed FA decrease in the right olfactory cortex. The cerebellum and CC, associated with typical motor impairment, showed the most consistent FA decreases in PD. Medication status, analysis approaches, and the number of diffusion directions have an important impact on the findings, needing careful evaluation in future meta-analyses.

**Keywords** Parkinson's disease; diffusion tensor imaging; fractional anisotropy; meta-analysis; anisotropic effect size–signed differential mapping

## Introduction

Parkinson's disease (PD) is the second most common neurodegenerative disease [1]. Clinically, PD is characterized by progressive motor symptoms, such as bradykinesia, rigidity, resting tremor, and postural instability, and various non-motor symptoms [2]. The pathophysiology of PD has yet to be fully elucidated, and this disease has no preventative or curative treatments. Recently, psychoradiology is emerging as the study of brain diseases through

a variety of non-invasive imaging techniques. Diffusion tensor imaging (DTI), a widely used magnetic resonance imaging (MRI) technique that visualizes and measures water diffusion, is particularly useful because of its high sensitivity to changes in white matter (WM) integrity [3]. Fractional anisotropy (FA), the most commonly used DTI parameter, is positively associated with WM anisotropy and can detect microstructural abnormalities of WM at very early stages [4,5].

Many DTI studies of PD have identified decreased FA in various brain regions, including corpus callosum (CC) [6–9], cerebellum [8,10–12], and superior and inferior longitudinal fasciculus (ILF) [9,10], but others have found no significant FA differences between patients with PD and healthy controls (HC) [13–15]. These discrepancies may

Received June 8, 2019; accepted October 12, 2019

Correspondence: Du Lei, leidu@ucmail.uc.edu;

Qiyong Gong, qiyonggong@hmrrc.org.cn

be attributable to factors such as small or heterogeneous study samples and methodological differences. To gain insights into the pathophysiology, a meta-analysis has a good chance of detecting consistent regions of FA alterations in PD.

Earlier reviews and meta-analyses confirmed that symptoms of PD are a result of the degeneration of the substantia nigra [16–18]. Although the pathologic process is mainly attributed to disruptions in the nigrostriatal dopamine system, previous neuroimaging studies in PD have focused on the substantia nigra using a seed-point method. By examining pre-defined regions of interest (ROI), some important cerebral alterations may have been missed. To overcome region placement preference bias, we chose a widely used whole-brain method to analyze the WM changes in PD. Previous DTI meta-analyses [19] did not directly test the hypothesis of WM changes in patients with PD compared with HC, and confounding factors such as medication status, disease stage, and methodological differences were not fully considered. A comprehensive meta-analysis is needed to explore the WM microstructure abnormalities and to investigate the effects of symptom severity and other clinical characteristics on regional WM alterations.

The aim of this meta-analysis was to define the most consistent WM microstructural changes, reflected by FA, in patients with PD using published whole brain DTI studies. To reduce the effects of heterogeneity, several subgroup analyses were conducted. Meta-regression analyses were used to evaluate the influence of clinical and demographic characteristics.

## Materials and methods

### Data sources, study selection, and quality assessment

This retrospective study was approved by the local institutional review committee. In accordance with the Preferred Reporting Items for Systematic Reviews and Meta-Analyses (PRISMA) statement [20], a comprehensive search of studies published before May 14, 2018 was conducted in the PubMed, Web of Science, and Embase databases using the keywords “Parkinson” OR “Parkinson’s disease” OR “PD”; AND “diffusion tensor” OR “diffusion tensor imaging” OR “DTI.” The references of these studies and relevant review articles were checked for additional relevant studies. Studies that satisfied the following conditions were included in the meta-analysis: (1) patients were diagnosed with idiopathic PD; (2) FA was compared between patients and HC; (3) three-dimensional coordinates (Montreal Neurological Institute (MNI) or Talairach) were reported for the whole-brain FA analysis; (4) significant results were reported using thresholds for

significance corrected for multiple comparisons or uncorrected with spatial extent thresholds; and (5) the study was published as an original article (not as a letter or abstract) in a peer-reviewed English-language journal. Data sets were excluded if they explicitly included patients diagnosed with comorbid neurological or psychiatric diseases (e.g., cognitive impairment or depression) [21]. To avoid sample overlaps: (1) for longitudinal studies, only baseline data were included [21]; (2) for studies reporting both on- and off-state results, only off-state data sets were included [21]; (3) for multiple studies using the same patient group, only the largest sample was included. Finally, the meta-analysis included 27 data sets from 24 studies with 808 patients with PD (429 men and 379 women) and 760 HC (393 men and 367 women) (Fig. 1).

Two of the authors independently rated each included study for quality and completeness using a 12-point checklist adapted from previous published meta-analyses [22] (Table S1). Any discrepancies were resolved by a third investigator.

### Voxel-wise meta-analysis

We analyzed FA differences in WM between patients with PD and HC using anisotropic effect size–signed differential mapping (AES-SDM), a voxel-based meta-analytic approach (see Supplementary Material). As detailed elsewhere [23–25], we extracted peak coordinates and effect sizes (e.g., *t*-values) of FA differences between patients with PD and HC from each data set. For each data set, we recreated a standard MNI map of FA differences using an anisotropic Gaussian kernel, from which the mean map was generated by voxel-wise calculation, weighted by sample size, intra-data set variability, and between-data set heterogeneity. To optimally balance false positive and negative findings, we used the default SDM kernel size and thresholds (full width at half maximum (FWHM) = 20 mm, uncorrected *P* = 0.005 was used as the main threshold, peak height *Z* = 1, cluster extent = 10 voxels) [23,24]. This FWHM kernel is intended to assign indicators of proximity to reported coordinates but not to smooth any image that is different in nature [25]. We adopted the tract-based spatial statistics (TBSS) template included in AES-SDM to allow the combination of voxel-based analysis (VBA) and TBSS studies [26]. We used MRICron software to visualize AES-SDM maps overlaid onto a high-resolution brain image template created by the International Consortium for Brain Mapping.

### Jackknife sensitivity analysis

Following preprocessing, we performed a whole-brain voxel-based jackknife sensitivity analysis to test the robustness of the findings by iteratively repeating the

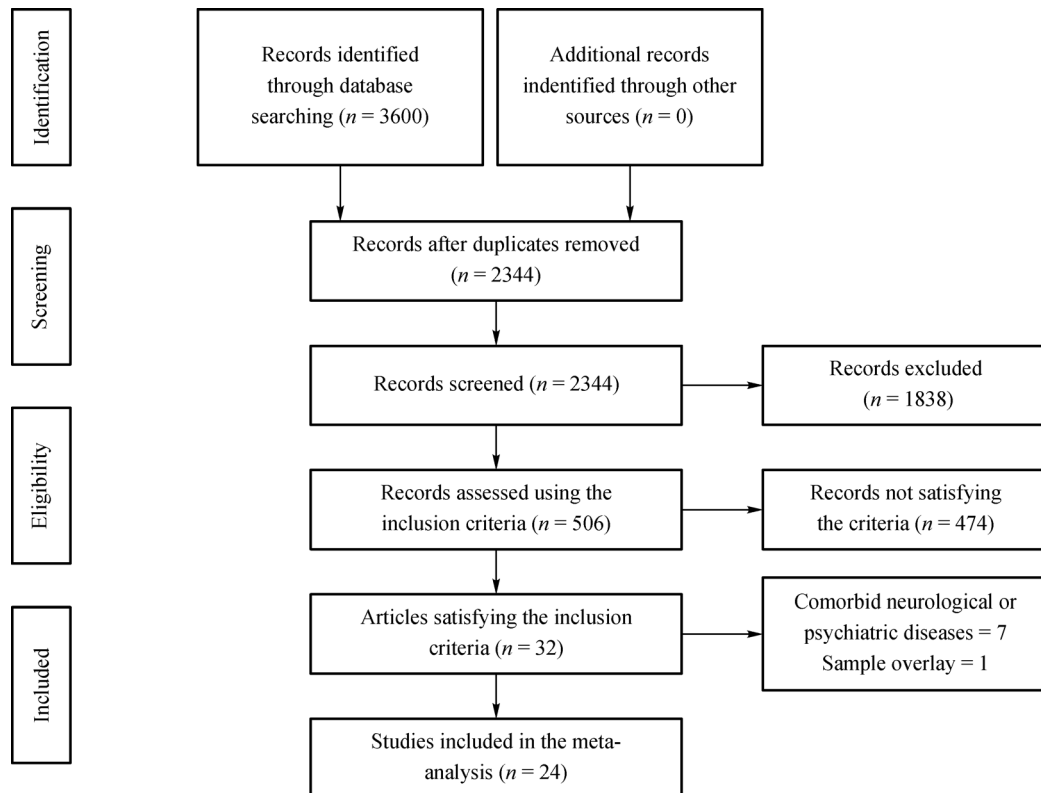


**Fig. 1** Flowchart describing the study selection for the meta-analysis.

analysis, excluding one data set each time. If a brain region remains significant in all or most of the combinations of studies, the finding is considered highly replicable [23].

### Analyses of heterogeneity and publication bias

We conducted a heterogeneity analysis using a random effects model with  $Q$  statistics to explore unexplained between-study variability in the results; heterogeneous brain regions were obtained using the default SDM kernel size and thresholds [25]. We also performed Egger's test for publication bias by extracting the values from statistically significant relevant peaks between patients with PD and HC [27].

### Subgroup analyses

Several subgroup meta-analyses were conducted to analyze clinical and methodological differences between these studies. This subgroup analysis included only studies with defined clinical and methodological homogeneity and was conducted for studies that investigated medicated and medication-free (including both medication-naïve and off-state) patients, studies that investigated early stage (Hoehn

and Yahr (H&Y) stage 1–2.5) patients [28], studies where the number of acquisition diffusion directions was  $\geq 30$  and  $< 30$  [29], and studies that used VBA or TBSS approaches.

### Meta-regression analyses

We used meta-regression analyses to examine the effects of age, percentage of female patients, illness duration, H&Y stage, Unified Parkinson's Disease Rating Scale (UPDRS) Part III score, and levodopa equivalent daily dose (LEDD) of patients with PD. We decreased the probability threshold to 0.0005 and cluster extent = 10 voxels, as described previously [26]. Regression plots were visually inspected to discard the fits driven by too few studies [23,24].

## Results

### Included studies and sample characteristics

The meta-analysis included 24 studies [6–15,30–43], and 3 of them included 2 independent databases [8,13,15], resulting in 27 data sets in all. Table 1 summarizes the

**Table 1** Demographic and clinical characteristics of participants in the 24 PD studies (27 data sets) included in the meta-analysis

Study	Sample (female)		Age (year)		UPDRS-III	H&Y stage	Duration (year)	Medication status	LEDD (mg/day)	Scanner	No. of directions	Software	Methods	Threshold	No. of coordinates	Quality scores (out of 12)
	PD	HC	PD	HC												
Guan <i>et al.</i> (2019) [30]	65 (33)	46 (25)	55.5	57.8	27.1	2.3	4.7	Off-state	NA	3.0T	15	FSL	TBSS	$P < 0.001$ , cluster-based corr	1	11
Wen <i>et al.</i> (2018) [31]	13 (3)	61 (20)	66.66	60.19	22.46	1.69	0.55	Drug-naïve	–	3.0T	64	FSL	TBSS	$P < 0.05$ , TFCE corr	0	10.5
Peran <i>et al.</i> (2018) [32]	26 (14)	26 (15)	63.8	66.0	19.1	<4	7.4	On-state	689	3.0T	32	FSL	VBA	$P < 0.01$ , TFCE corr	0	12
Rektor <i>et al.</i> (2018) [33]	20 (9)	21 (13)	61.9	57.9	NA	1–1.5	≤5	On-state	NA	3.0T	60	FSL	TBSS	$P < 0.05$ , TFCE corr	0	11.5
Acosta-Cabronero <i>et al.</i> (2017) [34]	25 (5)	50 (22)	63.6	63.6	16.3	2.2	6.0	On-state	748	3.0T	30	FSL	TBSS	$P < 0.001$ , uncorr	0	10.5
Chen <i>et al.</i> (2017) [6]	18 (11)	24 (13)	62.28	62.88	17.39	NA	3.06	Off-state	NA	3.0T	25	FSL	TBSS	$P < 0.017$ , TFCE & Bonferroni corr	2	11
Chen <i>et al.</i> (2017) [11]	29 (9)	26 (7)	61.51	60.11	27.03	2.36	NA	Off-state	NA	3.0T	13	FSL	VBA	$P < 0.05$ , AlphaSim corr	3	11
Chiang <i>et al.</i> (2017) [10]	66 (43)	67 (38)	58.1	56.8	22.74	1.98	3.86	On-state	279	3.0T	13	FSL	VBA	$P < 0.05$ , 3dClusterSim corr	6	11
Kamagata <i>et al.</i> (2017) [42]	30 (18)	28 (18)	67.6	66.5	16.1*	2.1	6.4	On-state	NA	3.0T	32	FSL	GBSS	$P < 0.05$ , TFCE corr	2	11.5
Luo <i>et al.</i> (2017) [13]	30 <sup>1</sup> (14)	26 (13)	53.42	54.46	25.37	1.60	2.00	Off-state	262	3.0T	25	FSL	TBSS	$P < 0.05$ , TFCE corr	0	11
	30 <sup>2</sup> (15)	26 (13)	52.55	54.46	22.27	1.63	2.35	Off-state	305	3.0T	25	FSL	TBSS	$P < 0.05$ , TFCE corr	0	11
Zanigni <i>et al.</i> (2017) [35]	47 (15)	27 (15)	66.5*	55.0*	NA	2.5*	2.8*	NA	NA	1.5T	25	FSL	TBSS	$P < 0.0038$ , TFCE & Bonferroni corr	0	10
Vervoort <i>et al.</i> (2016) [36]	16 (7)	19 (5)	55.1	58.1	28.9	1.94	4.87	Off-state	249	3.0T	61	FSL	TBSS	$P < 0.05$ , TFCE corr	0	10.5
Ji <i>et al.</i> (2015) [7]	20 (9)	20 (10)	64.20	59.95	32*	2*	5*	Off-state	NA	3.0T	30	FSL	TBSS	$P < 0.05$ , TFCE corr	1	11
Vercruyssen <i>et al.</i> (2015) [8]	11 <sup>3</sup> (3)	15 (4)	68.6	68.1	36.6	3*	9.5	On-state	704	3.0T	25/40/75	FSL	TBSS	$P < 0.05$ , FDR corr	1	11.5
	15 <sup>4</sup> (4)	15 (4)	67.6	68.1	32.5	2.5*	7.6	On-state	461	3.0T	25/40/75	FSL	TBSS	$P < 0.05$ , FDR corr	3	11.5
Agosta <i>et al.</i> (2014) [37]	13 (7)	33 (16)	63.9	64.0	28.3	2.4	10.0	On-state	567	1.5T	12	FSL	TBSS	$P < 0.05$ , TFCE corr	0	9.5

(Continued)

Study	Sample (female)		Age (year)		UPDRS- H&Y		Duration (year)	Medication status	LEDD (mg/day)	Scanner	No. of directions	Software	Methods	Threshold	No. of coordinates	Quality scores (out of 12)
	PD	HC	PD	HC	III	stage										
Worker <i>et al.</i> (2014) [14]	14 (7)	17 (8)	64.7	63.9	21.8	2.5*	6.6	On-state	NA	3.0T	64	FSL	TBSS	$P < 0.0167$ , TFCE & Bonferroni corr	0	11
Roskopf <i>et al.</i> (2014) [43]	15 (4)	18 (5)	67*	66*	26 <sup>#</sup>	NA	4*	NA	NA	1.5T	12	TIFT	WBSS	$P < 0.05$ , FDR corr	1	9.5
Agosta <i>et al.</i> (2013) [15]	63 <sup>5</sup> (22)	42 (17)	62.54	64	22.30	1–2.5	5.65	Off-state	NA	1.5T	12	FSL	TBSS	$P < 0.05$ , TFCE corr	0	9.5
	26 <sup>6</sup> (12)	42 (17)	65	64	40.92	3.46	12.38	Off-state	NA	1.5T	12	FSL	TBSS	$P < 0.05$ , TFCE corr	0	9.5
Kamagata <i>et al.</i> (2013) [38]	20 (12)	20 (10)	71.6	72.7	NA	2.4	7.83	On-state	464*	3.0T	32	FSL	TBSS	$P < 0.05$ , TFCE corr	0	10.5
Kim <i>et al.</i> (2013) [39]	64 (42)	64 (42)	62.9	63.0	NA	2*	5.3	Off-state	NA	3.0T	15	FSL	TBSS	$P < 0.05$ , TFCE corr	0	9.5
Melzer <i>et al.</i> (2013) [40]	63 (20)	32 (10)	64.0	70.1	25.3	2*	3.7	On-state	208	3.0T	28	FSL	TBSS	$P < 0.05$ , TFCE corr	0	11
Hattori <i>et al.</i> (2012) [41]	32 (20)	40 (22)	75.9	76.9	20	2.7	5.8	NA	NA	1.5T	12	FSL	TBSS	$P < 0.05$ , TFCE corr	0	9.5
Zhang <i>et al.</i> (2011) [12]	25 (14)	25 (14)	58.4	58.4	48 <sup>#</sup>	1–3	6.44	On-state	NA	3.0T	12	FSL	VBA	$P < 0.05$ , cluster-based corr	3	10.5
Karagulle Kendi <i>et al.</i> (2008) [9]	12 (7)	13 (5)	62.1	58.0	43.7 <sup>#</sup>	1.8	5.8	On-state	585	3.0T	12	SPM	VBA	$P < 0.05$ , corr for multiple comparison	18	11

PD, Parkinson's disease; HC, healthy controls; UPDRS, Unified Parkinson's Disease Rating Scale; H&Y, Hoehn and Yahr; NA, not available; LEDD, levodopa equivalent daily dose; SPM, statistical parametric mapping; FSL, functional MRI of the brain (fMRIB) software library; TBSS, tract-based spatial statistics; VBA, voxel-based analysis; TFCE, threshold-free cluster enhancement; FDR, false discovery rate; corr, corrected; uncorr, uncorrected; <sup>1</sup>patients with tremor-dominant; <sup>2</sup>patients with non-tremor-dominant; <sup>3</sup>patients with freezing of gait; <sup>4</sup>early and mild patients; <sup>5</sup>moderate and severe patients; \*Median; <sup>#</sup>UPDRS.

demographic, clinical, and imaging information of these studies, which provided a total of 41 coordinates of altered FA in patients with PD versus HC. Ten data sets from 8 studies and 13 data sets from 12 studies explicitly indicated patients in the medication off-state and on-state, and 1 study included medication-naïve patients. Three studies did not provide any information about the medication status (on- or off-state) at DTI acquisition. The patients recruited in 6 data sets from 5 studies were at their early stage. The number of acquisition diffusion directions was  $\geq 30$  in 11 data sets from 10 studies and  $< 30$  in 16 data sets from 14 studies. Seventeen studies used the TBSS approach, 5 used VBA, 1 used whole-brain-based spatial statistics, and 1 used gray-matter-based spatial statistics. Five of the 24 studies were performed on 1.5T scanners and 19 on 3T scanners. The quality scores, ranging from 9.5 to 12 (mean 10.7), demonstrated that the included studies were of high quality (Table 1).

### FA differences in the main meta-analysis

Meta-analysis revealed decreased FA in patients with PD relative to HC, in the left middle cerebellar peduncles (MCP), CC, left inferior fronto-occipital fasciculus (IFOF), and right ILF (Fig. 2, Table 2).

### Jackknife sensitivity analysis

Whole-brain jackknife sensitivity analysis showed that the most robust results were obtained for FA decreases in the WM regions of the left MCP and left CC, which were preserved throughout all combinations; right ILF and right CC were relatively replicable, being preserved throughout all but one combination; FA decreases in the left IFOF remained significant in all but two combinations (Table 3).

### Analyses of heterogeneity and publication bias

The left CC with altered FA had significant statistical heterogeneity among studies ( $P < 0.005$ ; Table 4). Egger's tests for publication bias were not significant with respect to FA differences in the left MCP ( $P = 0.107$ ), left CC ( $P = 0.122$ ), left IFOF ( $P = 0.126$ ), right CC ( $P = 0.059$ ), or right inferior longitudinal fasciculus ( $P = 0.057$ ) (Table 2).

### Subgroup analyses

The medication-free subgroup (comprising off-state ( $n = 10$  data sets) and medication-naïve patients ( $n = 1$  data set)) included 11 data sets comprising 374 patients with PD and

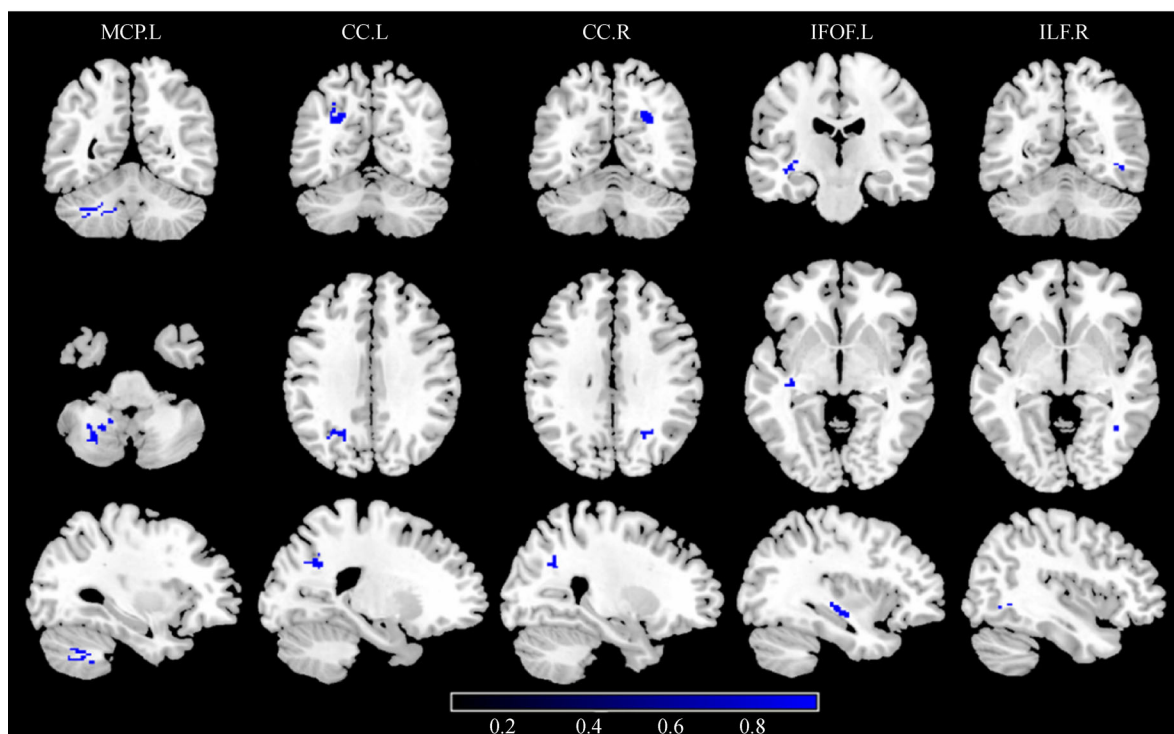


**Fig. 2** Regions showing reduced fractional anisotropy in patients with Parkinson's disease compared with healthy controls. CC, corpus callosum; IFOF, inferior fronto-occipital fasciculus; ILF, inferior longitudinal fasciculus; L, left; MCP, middle cerebellar peduncles; R, right.

**Table 2** Regional FA differences between patients with PD and HC identified by the present meta-analysis

Brain region (PD < HC)	MNI coordinates			SDM Z score	P value (uncorrected)	No. of voxels	Cluster breakdown (no. of voxels)	Egger's test (P value)
	X	Y	Z					
L middle cerebellar peduncles	-32	-54	-42	-1.412	0.000098109	221	Middle cerebellar peduncles (84) L cerebellum, crus I (9) L cerebellum, hemispheric lobule VIIIB (7) L cerebellum, hemispheric lobule VIII (7) L cerebellum, crus II (5) L cerebellum, hemispheric lobule VI (1) Undefined (108)	0.107
L corpus callosum	-22	-62	34	-1.754	~0	87	Corpus callosum (66) L superior longitudinal fasciculus II (11) L superior longitudinal fasciculus I (4) L inferior parietal (excluding supramarginal and angular) gyri, BA 7 (3) L middle occipital gyrus, BA 7 (3)	0.122
L inferior network, inferior fronto-occipital fasciculus	-36	-20	-4	-1.164	0.000784993	59	L inferior network, inferior fronto-occipital fasciculus (43) Undefined, BA 48 (12) Undefined, BA 20 (4)	0.126
R corpus callosum	26	-60	32	-1.251	0.000539660	29	Corpus callosum (29)	0.059
R inferior network, inferior longitudinal fasciculus	40	-58	-4	-1.204	0.000637770	16	R inferior network, inferior longitudinal fasciculus (12) Right inferior temporal gyrus, BA 37 (4)	0.057

BA, Brodmann area; FA, fractional anisotropy; HC, healthy controls; L, left; MNI, Montreal Neurological Institute; PD, Parkinson's disease; R, right; SDM, signed differential mapping.

328 HC. The analysis revealed FA decreases in the right olfactory cortex. The medicated group ( $n = 13$  data sets) comprised 340 patients with PD and 347 HC. The main results remained unchanged. We then used a threshold of LEDD = 400 mg/day to define two medicated subgroups. In the LEDD < 400 mg/day subgroup analysis ( $n = 5$  data sets), comprising 205 patients with PD and 144 HC, the main results remained unchanged; by contrast, the LEDD  $\geq$  400 mg/day subgroup ( $n = 7$  data sets), comprising 122 patients with PD and 157 HC, revealed FA increases in the bilateral CC.

In the early stage disease ( $n = 6$  data sets) and VBA ( $n = 5$  data sets) subgroups, the main results remained unchanged, but the TBSS ( $n = 20$  data sets) subgroup analysis failed to detect between-group differences. In the

< 30 diffusion directions subgroup analysis ( $n = 16$  data sets), four of the main results remain unchanged, whereas the  $\geq$  30 diffusion directions subgroup ( $n = 11$  data sets) only revealed one main result in the left IFOF. Detailed results of subgroup analyses are shown in Table 5 and Figs. S1–S6.

### Meta-regression analyses

The mean age of patients, percentage of women with PD (in the whole PD group in each study), mean illness duration, mean H&Y stage, mean UPDRS-III score, and mean LEDD of patients with PD were not significantly associated with PD-related WM FA changes, at least linearly.

**Table 3** Jackknife sensitivity analysis\*

Discarded study	Left middle cerebellar peduncles	Left corpus callosum	Right corpus callosum	Left inferior network, inferior fronto-occipital fasciculus	Right inferior network, inferior longitudinal fasciculus
Guan <i>et al.</i> (2019) [30]	Yes	Yes	Yes	Yes	Yes
Wen <i>et al.</i> (2018) [31]	Yes	Yes	Yes	Yes	Yes
Peran <i>et al.</i> (2018) [32]	Yes	Yes	Yes	Yes	Yes
Rektor <i>et al.</i> (2018) [33]	Yes	Yes	Yes	Yes	Yes
Acosta-Cabronero <i>et al.</i> (2017) [34]	Yes	Yes	Yes	Yes	Yes
Chen <i>et al.</i> (2017) [6]	Yes	Yes	Yes	Yes	Yes
Chen <i>et al.</i> (2017) [11]	Yes	Yes	Yes	Yes	Yes
Chiang <i>et al.</i> (2017) [10]	Yes	Yes	No	No	No
Kamagata <i>et al.</i> (2017) [42]	Yes	Yes	Yes	No	Yes
Luo <i>et al.</i> (2017) <sup>a</sup> [13]	Yes	Yes	Yes	Yes	Yes
	Yes	Yes	Yes	Yes	Yes
Zanigni <i>et al.</i> (2017) [35]	Yes	Yes	Yes	Yes	Yes
Vervoort <i>et al.</i> (2016) [36]	Yes	Yes	Yes	Yes	Yes
Ji <i>et al.</i> (2015) [7]	Yes	Yes	Yes	Yes	Yes
Vercruyse <i>et al.</i> (2015) <sup>a</sup> [8]	Yes	Yes	Yes	Yes	Yes
	Yes	Yes	Yes	Yes	Yes
Agosta <i>et al.</i> (2014) [37]	Yes	Yes	Yes	Yes	Yes
Worker <i>et al.</i> (2014) [14]	Yes	Yes	Yes	Yes	Yes
Roskopf <i>et al.</i> (2014) [43]	Yes	Yes	Yes	Yes	Yes
Agosta <i>et al.</i> (2013) <sup>a</sup> [15]	Yes	Yes	Yes	Yes	Yes
	Yes	Yes	Yes	Yes	Yes
Kamagata <i>et al.</i> (2013) [38]	Yes	Yes	Yes	Yes	Yes
Kim <i>et al.</i> (2013) [39]	Yes	Yes	Yes	Yes	Yes
Melzer <i>et al.</i> (2013) [40]	Yes	Yes	Yes	Yes	Yes
Hattori <i>et al.</i> (2012) [41]	Yes	Yes	Yes	Yes	Yes
Zhang <i>et al.</i> (2011) [12]	Yes	Yes	Yes	Yes	Yes
Karagulle Kendi <i>et al.</i> (2008) [9]	Yes	Yes	Yes	Yes	Yes
Total	27 out of 27	27 out of 27	26 out of 27	25 out of 27	26 out of 27

<sup>a</sup> two data sets included.

\* “Yes” indicates that the specific region of FA reduction was significant in the specific jackknife analysis; “No” indicates that the specific region of FA reduction was not significant in specific analysis.

**Table 4** Regions of FA heterogeneity from the SDM analysis

Brain region	MNI coordinates			SDM Z score	P value (uncorrected)	No. of voxels	Cluster breakdown (no. of voxels)
	X	Y	Z				
Corpus callosum	-26	-62	32	1.911	0.000073612	12	Corpus callosum (12)

FA, fractional anisotropy; MNI, Montreal Neurological Institute; SDM, signed differential mapping.

## Discussion

### The main abnormalities and their potential significance

Our pooled meta-analysis of DTI studies revealed significant WM microarchitecture alterations in patients with PD compared with HC as indicated by the decreased FA values. A consistent decrease in FA was observed in the left MCP, CC, left IFOF, and right ILF. Jackknife

sensitivity analysis, heterogeneity analysis, and Egger’s tests confirmed the robustness of these findings. Although the subgroup analysis of medication-free patients did not reveal decreased FA as in the main analysis, it detected an additional cluster in the right olfactory cortex. Meta-regression analyses revealed no significant association between WM alterations and relevant demographic and clinical variables.

Given the role of the MCP as the main afferent pathway

**Table 5** Subgroup meta-analysis of studies in patients with PD compared with HC

	Brain region (PD<HC)	MNI coordinates			SDMZ score	P value (uncorrected)	No. of voxels
		X	Y	Z			
Medication-free patients	R olfactory cortex, BA 48	22	12	-18	-1.156	0.000049055	50
Medicated patients	L middle cerebellar peduncles	-34	-54	-44	-1.645	0.000296830	65
	L corpus callosum	-24	-62	28	-1.647	0.000220776	61
	L inferior network, inferior fronto-occipital fasciculus	-36	-20	-4	-1.662	0.000196218	54
	R corpus callosum	24	-60	32	-1.645	0.000269830	31
	R inferior network, inferior longitudinal fasciculus	42	-58	-6	-1.630	0.000318885	17
LEDD $\geq$ 400 mg	R corpus callosum	4	-14	26	1.122	0.000049055	146
	L corpus callosum	-22	-38	28	1.060	0.000343442	65
LEDD < 400 mg	L middle cerebellar peduncles	-30	-54	-38	-1.496	0.000073612	71
	R corpus callosum	28	-62	28	-1.495	0.000073612	31
	L corpus callosum	-20	-62	32	-1.457	0.000392497	23
	L inferior network, inferior fronto-occipital fasciculus	-34	-20	-2	-1.486	0.000171721	21
	R inferior network, inferior longitudinal fasciculus	44	-54	-6	-1.481	0.000269830	12
Early stage patients	L middle cerebellar peduncles	-34	-58	-38	-1.473	0.000024557	76
	R corpus callosum	22	-60	34	-1.467	0.000098109	31
	L middle occipital gyrus, BA 7	-30	-68	38	-1.458	0.000196218	30
	L corpus callosum	-20	-60	34	-1.465	0.000122666	20
	L inferior network, inferior fronto-occipital fasciculus	-36	-20	-4	-1.445	0.000269830	15
	R inferior network, inferior longitudinal fasciculus	42	-64	-6	-1.458	0.000196218	12
TBSS	None						
VBA	L middle cerebellar peduncles	-40	-56	-38	-2.350	~0	263
	L corpus callosum	-28	-64	26	-2.341	~0	97
	R corpus callosum	24	-58	30	-1.721	0.000515163	24
	L inferior network, inferior fronto-occipital fasciculus	-36	-20	-4	-1.667	0.001030266	12
	R inferior network, inferior longitudinal fasciculus	44	-56	-6	-1.702	0.000662327	10
Number of diffusion directions $\geq$ 30	L inferior network, inferior fronto-occipital fasciculus	-36	-14	-10	-1.133	0.000073612	66
Number of diffusion directions < 30	L middle cerebellar peduncles	-32	-54	-42	-1.682	0.000024557	224
	L corpus callosum	-28	-62	28	-1.683	0.000024557	87
	R corpus callosum	26	-60	30	-1.357	0.000343442	29
	R inferior network, inferior longitudinal fasciculus	40	-56	-4	-1.334	0.000539660	16
	L inferior network, inferior fronto-occipital fasciculus	-36	-20	-4	-1.023	0.002551138	10

BA, Brodmann area; HC, healthy controls; L, left; MNI, Montreal Neurological Institute; PD, Parkinson's disease; R, right; SDM, signed differential mapping; TBSS, tract-based spatial statistics; VBA, voxel-based analysis.

from the cortex to the cerebellum and additional findings of diffusion changes in brainstem and pons [44], these data emphasize the role of the cortico-ponto-cerebellar loop in PD pathology. This loop contains afferent axons from the pontine nuclei [45] and mediates complex brain functions concerning movement and cognition. PD features motor dysfunction such as tremor, rigidity, bradykinesia, gait disturbance, and postural instability [46]. Studies of patients with freezing of gait found WM abnormalities in the pontine-cerebellar tracts [8,47,48], which might explain their reduced ability to recruit the cerebellum. Functional studies in PD found hypoactivation in the cerebellum during a motor task [49]. This neurodegeneration in MCP is consistent with the critical role of the cerebellum for motor performance [46,50]. Moreover, the subgroup analysis of PD patients with early stage disease detected decreased FA in MCP, an area with a significant decline in diffusivity in early PD, correlating with motor progression [51].

Being the largest WM bundle in the human brain, the CC connects the bilateral cerebral hemispheres [52]; therefore, this finding, suggesting hemispheric involvement [53], is consistent with resting-state studies reporting decreased interhemispheric functional connectivity in PD [54–56]. In previous DTI studies in PD, altered FA was reported in different subdivisions of the CC, such as the genu, which is usually associated with cognitive impairment [37,38,57]. Microstructural impairment of CC has been reported in cognitively normal patients with PD, which points toward an affected interhemispheric connectivity that possibly shapes the onset of cognitive deficits [58]. In our meta-analysis, the abnormal microstructure of the posterior CC was detected in the pooled analysis and the subgroups of patients with early stage disease, medicated patients, VBA method, and < 30 diffusion directions; this finding is consistent with reports of a smaller posterior CC volume in patients with PD [59]. Transcallosal motor fiber bundles cross the CC in the posterior part [60]. The anatomic projections found in this study are compatible with previous observations that CC abnormalities are related to postural instability and freezing of gait in PD [60], which becomes more severe with motor worsening [61]. Thus, the importance of neurodegeneration of CC in PD is also reflected through its role in motor features of the disease.

The ILF is an associative bundle connecting the occipital and temporal lobes. Its long fibers connect visual areas to the amygdala and hippocampus, the main components of the limbic system related to emotional behavior [62]. It is involved in face recognition [63], visual perception [64], and visual memory [65]. The IFOF is a ventral associative bundle connecting the ventral occipital lobe and the orbitofrontal cortex [66]. Its occipital component runs parallel to the ILF. On approaching the anterior temporal lobe, its fibers gather together and enter the external

capsule dorsally to the fasciculus. The IFOF is involved in reading [67] and visual processing [68]. The functions of these two bundles are not yet completely understood in PD. Guan and colleagues found that the ILF is associated with motor impairment and global disease severity in PD [30], which has also been reported in relation to the tremor-dominant (TD) subtype of PD, indicating probably different underlying pathologies between TD and other motor subtypes [69]. FA values in the IFOF were negatively correlated with bradykinesia of PD [70], and disruption of this structure might contribute to freezing of gait due to impaired visuospatial processing [71]. However, a recent DTI study showed significant differences in these two bundles between patients with postural instability gait disorder and HC [72]. The role of these two bundles in differentiating WM changes in PD motor subtypes requires further investigation. Notably, previous studies also found relationships between these two bundles and non-motor symptoms of PD, such as depression [73] and cognitive dysfunction [74]. Although studies with comorbid depression and cognitive dysfunction were excluded in the current meta-analysis, the potentially confounding effects could not be completely ruled out. Moreover, although detailed depression scales were not used in these included studies, depression is a frequent non-motor symptom in patients with PD, and its prevalence can be as high as 90% [75].

The quantitative statistical meta-analyses have been carried out on DTI studies in PD [17]. Although these earlier meta-analyses provide valuable insights into the underlying WM pathology, differences in the ROI placement likely result in significant heterogeneity between studies. Relative to ROI-based analyses, coordinate-based analyses are less susceptible to errors relating to the lack of spatial distinction [76]. There is relatively poor consistency of results between previous ROI meta-analyses and our current coordinate-based meta-analysis, which has implications for neuroimaging meta-analyses of other disorders, such as amnesic mild cognitive impairment [76] and post-traumatic stress disorder [77]. Several factors might contribute to these differences. First, ROI studies typically report on a subset of brain regions and are likely to suffer from publication bias. Second, where seed-based mapping uses coordinate data, the effect size is biased toward zero in brain regions where there are no significant clusters.

### Subgroup analyses

The subgroup analysis of medication-free patients detected a cluster in the right olfactory cortex, which is considered an early affected site in the Braak model of temporal degeneration in PD [78]. A recent DTI study suggested that olfactory regions were particularly efficient at distinguishing drug-naïve patients with PD from HC [79]. There is

evidence of a strong link between olfactory discrimination and orbitofrontal cortex [80]. Decreased FA in the olfactory cortex may be related to the olfactory dysfunction, which is present in ~90% of early stage PD [81]. However, we did not observe this alteration in the olfactory cortex in the pooled whole-group results. The reason for this discrepancy is unclear, although changes associated with medication may normalize, or at least obscure, the intrinsic changes in these regions. Medication exposure is an important potential confounder, and understanding the effect of medications on white-matter abnormalities in patients with PD is critical for the interpretation of results. In functional MRI studies, levodopa can normalize altered functional connectivity in PD [82]. Medications have also been shown to affect cerebral WM; for example, benzotropine used in the treatment of tremor in PD promotes re-myelination [83]. In the current meta-analysis, the main results of the LEDD < 400 mg/day subgroup analysis remain unchanged, whereas the results of the LEDD  $\geq$  400 mg/day subgroup show increased FA in the bilateral CC, sharing these two clusters with the results of the pooled meta-analysis. This observation seems to fit a “normalization” effect. Although other diffusion MRI studies have shown that medication *per se* has little influence on WM integrity or does not alter diffusion [38,84], the effect of dopaminergic medication on WM is still unclear. The differential influence of dopamine medication is likely determined by additional factors. Inter-individual differences and disease severity should also be considered. Further studies that are specifically designed to detect the effect of medication exposure on WM changes in patients with PD are needed.

Scan acquisition parameters also affect FA measurements individually and in group comparisons. The minimum requirement for a qualitative DTI calculation is 6 non-collinear diffusion directions, whereas robust estimation of FA and tensor orientation requires at least 30 unique and evenly distributed sampling orientations [29]. DTI studies with less than 30 diffusion directions tend to overestimate FA values, possibly affecting group-wise differences. However, our subgroup analysis of  $\geq$  30 diffusion directions showed the same robust decrease in FA in the left IFOF as in the main analysis. Nevertheless, future DTI meta-analyses should consider the number of diffusion directions.

Subgroup analysis of the VBA studies revealed clusters that were identified in the pooled analysis; however, the subgroup analysis of the TBSS studies did not. This difference may be a methodological issue. TBSS was developed to analyze diffusion data, and it isolates the central core of WM tracts with the highest FA and reports significant clusters within that WM skeleton [85]; however, it may miss abnormalities in the peripheral WM [86]. VBA investigates the integrity of all WM voxels, including peripheral regions of WM and fiber crossings [87].

Differences in findings between the two methods are thus to be expected. Moreover, given the small number of VBA studies ( $n = 5$ ), we cannot completely rule out the possibility of chance findings.

### Limitations of this study

First, methodological heterogeneity cannot be completely excluded: it was impossible to perform analyses or subgroup analyses of all relevant variables. Second, the medication-free patients of subgroup meta-analysis were mostly medicated patients in the off-state at scanning. Clearly, the best way to minimize the effects of treatment is to study medication-naïve patients; however, this subgroup was small. The results of the subgroup meta-analysis for medication-free data sets should therefore be interpreted with caution, considering the possible methodological differences between the studies, such as diffusion directions and analysis methods. Third, as is inherent in all coordinate-based methods, our meta-analysis used the coordinates from the included studies rather than the original t-statistic maps, which somewhat limits the accuracy of the results. Fourth, although we performed several subgroup meta-analyses, including VBA and different LEDD medicated data sets, for the early stage, the results should be interpreted with caution. The small sample size of these subgroup meta-analyses limits the generalizability of the results.

In conclusion, this meta-analysis demonstrates a consistent pattern of decreased FA in the left MCP, CC, IFOF, and ILF. In particular, FA decreases in the MCP and CC in PD were robustly present in the sensitivity analyses. These results suggest that the altered WM microstructures in the MCP and CC may serve as a potential neuroimaging biomarker of PD. Furthermore, the subgroup analyses show that medication status, analysis approaches, and the number of diffusion directions have an important impact on the findings, which should be treated with caution in future meta-analysis studies.

### Acknowledgements

This study was supported by the National Natural Science Foundation (Nos. 81621003, 81761128023, 81220108013, 81227002, and 81030027), the Program for Innovative Research Team in University (No. IRT16R52) of China, the Professorship Award (No. T2014190) of China, and the CMB Distinguished Professorship Award (No. F510000/G16916411) administered by the Institute of International Education.

### Compliance with ethics guidelines

Xueling Suo, Du Lei, Wenbin Li, Lei Li, Jing Dai, Song Wang, Nannan Li, Lan Cheng, Rong Peng, Graham J Kemp, and Qiyong Gong declare that they have no conflict of interest. All procedures

followed were in accordance with the ethical standards of the responsible committee on human experimentation (institutional and national) and with the *Helsinki Declaration* of 1975, as revised in 2000 (5). Informed consent was obtained from all patients for being included in the study.

**Electronic Supplementary Material** Supplementary material is available in the online version of this article at <https://doi.org/10.1007/s11684-019-0725-5> and is accessible for authorized users.

## References

- de Lau LM, Breteler MM. Epidemiology of Parkinson's disease. *Lancet Neurol* 2006; 5(6): 525–535
- Reichmann H, Brandt MD, Klingelhoefer L. The nonmotor features of Parkinson's disease: pathophysiology and management advances. *Curr Opin Neurol* 2016; 29(4): 467–473
- Kubicki M, Westin CF, Maier SE, Mamata H, Frumin M, Ersner-Hersfield H, Kikinis R, Jolesz FA, McCarley R, Shenton ME. Diffusion tensor imaging and its application to neuropsychiatric disorders. *Harv Rev Psychiatry* 2002; 10(6): 324–336
- Taylor WD, Hsu E, Krishnan KR, MacFall JR. Diffusion tensor imaging: background, potential, and utility in psychiatric research. *Biol Psychiatry* 2004; 55(3): 201–207
- Le Bihan D, Mangin JF, Poupon C, Clark CA, Pappata S, Molko N, Chabriat H. Diffusion tensor imaging: concepts and applications. *J Magn Reson Imaging* 2001; 13(4): 534–546
- Chen B, Fan G, Sun W, Shang X, Shi S, Wang S, Lv G, Wu C. Usefulness of diffusion-tensor MRI in the diagnosis of Parkinson variant of multiple system atrophy and Parkinson's disease: a valuable tool to differentiate between them? *Clin Radiol* 2017; 72(7): 610.e9–610.e15
- Ji L, Wang Y, Zhu D, Liu W, Shi J. White matter differences between multiple system atrophy (parkinsonian type) and Parkinson's disease: a diffusion tensor image study. *Neuroscience* 2015; 305: 109–116
- Vercruyse S, Leunissen I, Vervoort G, Vandenbergh W, Swinnen S, Nieuwboer A. Microstructural changes in white matter associated with freezing of gait in Parkinson's disease. *Mov Disord* 2015; 30(4): 567–576
- Karagulle Kendi AT, Lehericy S, Luciana M, Ugurbil K, Tuite P. Altered diffusion in the frontal lobe in Parkinson disease. *AJNR Am J Neuroradiol* 2008; 29(3): 501–505
- Chiang PL, Chen HL, Lu CH, Chen PC, Chen MH, Yang IH, Tsai NW, Lin WC. White matter damage and systemic inflammation in Parkinson's disease. *BMC Neurosci* 2017; 18(1): 48
- Chen MH, Chen PC, Lu CH, Chen HL, Chao YP, Li SH, Chen YW, Lin WC. Plasma DNA mediate autonomic dysfunctions and white matter injuries in patients with Parkinson's disease. *Oxid Med Cell Longev* 2017; 2017: 7371403
- Zhang K, Yu C, Zhang Y, Wu X, Zhu C, Chan P, Li K. Voxel-based analysis of diffusion tensor indices in the brain in patients with Parkinson's disease. *Eur J Radiol* 2011; 77(2): 269–273
- Luo C, Song W, Chen Q, Yang J, Gong Q, Shang HF. White matter microstructure damage in tremor-dominant Parkinson's disease patients. *Neuroradiology* 2017; 59(7): 691–698
- Worker A, Blain C, Jarosz J, Chaudhuri KR, Barker GJ, Williams SC, Brown RG, Leigh PN, Dell'Acqua F, Simmons A. Diffusion tensor imaging of Parkinson's disease, multiple system atrophy and progressive supranuclear palsy: a tract-based spatial statistics study. *PLoS One* 2014; 9(11): e112638
- Agosta F, Canu E, Stojković T, Pievani M, Tomić A, Sarro L, Dragašević N, Copetti M, Comi G, Kostić VS, Filippi M. The topography of brain damage at different stages of Parkinson's disease. *Hum Brain Mapp* 2013; 34(11): 2798–2807
- Schwarz ST, Abaei M, Gontu V, Morgan PS, Bajaj N, Auer DP. Diffusion tensor imaging of nigral degeneration in Parkinson's disease: a region-of-interest and voxel-based study at 3 T and systematic review with meta-analysis. *Neuroimage Clin* 2013; 3: 481–488
- Atkinson-Clement C, Pinto S, Eusebio A, Coulon O. Diffusion tensor imaging in Parkinson's disease: review and meta-analysis. *Neuroimage Clin* 2017; 16: 98–110
- Cochrane CJ, Ebmeier KP. Diffusion tensor imaging in parkinsonian syndromes: a systematic review and meta-analysis. *Neurology* 2013; 80(9): 857–864
- Albrecht F, Ballarini T, Neumann J, Schroeter ML. FDG-PET hypometabolism is more sensitive than MRI atrophy in Parkinson's disease: a whole-brain multimodal imaging meta-analysis. *Neuroimage Clin* 2019; 21: 101594
- Moher D, Liberati A, Tetzlaff J, Altman DG; PRISMA Group. Preferred reporting items for systematic reviews and meta-analyses: the PRISMA statement. *PLoS Med* 2009; 6(7): e1000097
- Pan P, Zhan H, Xia M, Zhang Y, Guan D, Xu Y. Aberrant regional homogeneity in Parkinson's disease: a voxel-wise meta-analysis of resting-state functional magnetic resonance imaging studies. *Neurosci Biobehav Rev* 2017; 72: 223–231
- Shepherd AM, Matheson SL, Laurens KR, Carr VJ, Green MJ. Systematic meta-analysis of insula volume in schizophrenia. *Biol Psychiatry* 2012; 72(9): 775–784
- Radua J, Mataix-Cols D. Voxel-wise meta-analysis of grey matter changes in obsessive-compulsive disorder. *Br J Psychiatry* 2009; 195(5): 393–402
- Radua J, Mataix-Cols D, Phillips ML, El-Hage W, Kronhaus DM, Cardoner N, Surguladze S. A new meta-analytic method for neuroimaging studies that combines reported peak coordinates and statistical parametric maps. *Eur Psychiatry* 2012; 27(8): 605–611
- Radua J, Rubia K, Canales-Rodríguez EJ, Pomarol-Clotet E, Fusar-Poli P, Mataix-Cols D. Anisotropic kernels for coordinate-based meta-analyses of neuroimaging studies. *Front Psychiatry* 2014; 5: 13
- Wise T, Radua J, Nortje G, Cleare AJ, Young AH, Arnone D. Voxel-based meta-analytical evidence of structural disconnectivity in major depression and bipolar disorder. *Biol Psychiatry* 2016; 79(4): 293–302
- Radua J, Grau M, van den Heuvel OA, Thiebaut de Schotten M, Stein DJ, Canales-Rodríguez EJ, Catani M, Mataix-Cols D. Multimodal voxel-based meta-analysis of white matter abnormalities in obsessive-compulsive disorder. *Neuropsychopharmacology* 2014; 39(7): 1547–1557
- Chen S, Chan P, Sun S, Chen H, Zhang B, Le W, Liu C, Peng G, Tang B, Wang L, Cheng Y, Shao M, Liu Z, Wang Z, Chen X, Wang M, Wan X, Shang H, Liu Y, Xu P, Wang J, Feng T, Chen X, Hu X,

- Xie A, Xiao Q. The recommendations of Chinese Parkinson's disease and movement disorder society consensus on therapeutic management of Parkinson's disease. *Transl Neurodegener* 2016; 5 (1): 12
29. Jones DK. The effect of gradient sampling schemes on measures derived from diffusion tensor MRI: a Monte Carlo study. *Magn Reson Med* 2004; 51(4): 807–815
30. Guan X, Huang P, Zeng Q, Liu C, Wei H, Xuan M, Gu Q, Xu X, Wang N, Yu X, Luo X, Zhang M. Quantitative susceptibility mapping as a biomarker for evaluating white matter alterations in Parkinson's disease. *Brain Imaging Behav* 2019; 13(1): 220–231
31. Wen MC, Heng HSE, Lu Z, Xu Z, Chan LL, Tan EK, Tan LCS. Differential white matter regional alterations in motor subtypes of early drug-naive Parkinson's disease patients. *Neurorehabil Neural Repair* 2018; 32(2): 129–141
32. Péran P, Barbagallo G, Nemmi F, Sierra M, Galitzky M, Traon AP, Payoux P, Meissner WG, Rascol O. MRI supervised and unsupervised classification of Parkinson's disease and multiple system atrophy. *Mov Disord* 2018; 33(4): 600–608
33. Rektor I, Svátková A, Vojtíšek L, Zikmundová I, Vaniček J, Király A, Szabó N. White matter alterations in Parkinson's disease with normal cognition precede grey matter atrophy. *PLoS One* 2018; 13 (1): e0187939
34. Acosta-Cabronero J, Cardenas-Blanco A, Betts MJ, Butryn M, Valdes-Herrera JP, Galazky I, Nestor PJ. The whole-brain pattern of magnetic susceptibility perturbations in Parkinson's disease. *Brain* 2017; 140(1): 118–131
35. Zanigni S, Evangelisti S, Testa C, Manners DN, Calandra-Buonaura G, Guarino M, Gabellini A, Gramegna LL, Giannini G, Sambati L, Cortelli P, Lodi R, Tonon C. White matter and cortical changes in atypical parkinsonisms: a multimodal quantitative MR study. *Parkinsonism Relat Disord* 2017; 39: 44–51
36. Vervoort G, Leunissen I, Firbank M, Heremans E, Nackaerts E, Vandenberghe W, Nieuwboer A. Structural brain alterations in motor subtypes of Parkinson's disease: evidence from probabilistic tractography and shape analysis. *PLoS One* 2016; 11(6): e0157743
37. Agosta F, Canu E, Stefanova E, Sarro L, Tomić A, Špica V, Comi G, Kostić VS, Filippi M. Mild cognitive impairment in Parkinson's disease is associated with a distributed pattern of brain white matter damage. *Hum Brain Mapp* 2014; 35(5): 1921–1929
38. Kamagata K, Motoi Y, Tomiyama H, Abe O, Ito K, Shimoji K, Suzuki M, Hori M, Nakanishi A, Sano T, Kuwatsuru R, Sasai K, Aoki S, Hattori N. Relationship between cognitive impairment and white-matter alteration in Parkinson's disease with dementia: tract-based spatial statistics and tract-specific analysis. *Eur Radiol* 2013; 23(7): 1946–1955
39. Kim HJ, Kim SJ, Kim HS, Choi CG, Kim N, Han S, Jang EH, Chung SJ, Lee CS. Alterations of mean diffusivity in brain white matter and deep gray matter in Parkinson's disease. *Neurosci Lett* 2013; 550: 64–68
40. Melzer TR, Watts R, MacAskill MR, Pitcher TL, Livingston L, Keenan RJ, Dalrymple-Alford JC, Anderson TJ. White matter microstructure deteriorates across cognitive stages in Parkinson disease. *Neurology* 2013; 80(20): 1841–1849
41. Hattori T, Orimo S, Aoki S, Ito K, Abe O, Amano A, Sato R, Sakai K, Mizusawa H. Cognitive status correlates with white matter alteration in Parkinson's disease. *Hum Brain Mapp* 2012; 33(3): 727–739
42. Kamagata K, Zalesky A, Hatano T, Ueda R, Di Biase MA, Okuzumi A, Shimoji K, Hori M, Caeyenberghs K, Pantelis C, Hattori N, Aoki S. Gray matter abnormalities in idiopathic Parkinson's disease: evaluation by diffusional kurtosis imaging and neurite orientation dispersion and density imaging. *Hum Brain Mapp* 2017; 38(7): 3704–3722
43. Roskopf J, Müller HP, Huppertz HJ, Ludolph AC, Pinkhardt EH, Kassubek J. Frontal corpus callosum alterations in progressive supranuclear palsy but not in Parkinson's disease. *Neurodegener Dis* 2014; 14(4): 184–193
44. Ziegler E, Rouillard M, André E, Coolen T, Stender J, Balteau E, Phillips C, Garraux G. Mapping track density changes in nigrostriatal and extranigral pathways in Parkinson's disease. *Neuroimage* 2014; 99: 498–508
45. Stoodley CJ, Schmahmann JD. Evidence for topographic organization in the cerebellum of motor control versus cognitive and affective processing. *Cortex* 2010; 46(7): 831–844
46. Wu T, Hallett M. The cerebellum in Parkinson's disease. *Brain* 2013; 136(3): 696–709
47. Schweder PM, Hansen PC, Green AL, Quaghebeur G, Stein J, Aziz TZ. Connectivity of the pedunculopontine nucleus in parkinsonian freezing of gait. *Neuroreport* 2010; 21(14): 914–916
48. Canu E, Agosta F, Sarasso E, Volontè MA, Basaia S, Stojkovic T, Stefanova E, Comi G, Falini A, Kostic VS, Gatti R, Filippi M. Brain structural and functional connectivity in Parkinson's disease with freezing of gait. *Hum Brain Mapp* 2015; 36(12): 5064–5078
49. Tessa C, Lucetti C, Diciotti S, Paoli L, Cecchi P, Giannelli M, Baldacci F, Ginestroni A, Vignali C, Mascalchi M, Bonuccelli U. Hypoactivation of the primary sensorimotor cortex in *de novo* Parkinson's disease: a motor fMRI study under controlled conditions. *Neuroradiology* 2012; 54(3): 261–268
50. Hall JM, Ehgoetz Martens KA, Walton CC, O'Callaghan C, Keller PE, Lewis SJ, Moustafa AA. Diffusion alterations associated with Parkinson's disease symptomatology: a review of the literature. *Parkinsonism Relat Disord* 2016; 33: 12–26
51. Sobhani S, Rahmani F, Aarabi MH, Sadr AV. Exploring white matter microstructure and olfaction dysfunction in early Parkinson disease: diffusion MRI reveals new insight. *Brain Imaging Behav* 2019; 13(1): 210–219
52. Catani M, Howard RJ, Pajevic S, Jones DK. Virtual *in vivo* interactive dissection of white matter fasciculi in the human brain. *Neuroimage* 2002; 17(1): 77–94
53. Cronin-Golomb A. Parkinson's disease as a disconnection syndrome. *Neuropsychol Rev* 2010; 20(2): 191–208
54. Hu X, Zhang J, Jiang X, Zhou C, Wei L, Yin X, Wu Y, Li J, Zhang Y, Wang J. Decreased interhemispheric functional connectivity in subtypes of Parkinson's disease. *J Neurol* 2015; 262(3): 760–767
55. Luo C, Guo X, Song W, Zhao B, Cao B, Yang J, Gong Q, Shang HF. Decreased resting-state interhemispheric functional connectivity in Parkinson's disease. *BioMed Res Int* 2015; 2015: 692684
56. Li J, Yuan Y, Wang M, Zhang J, Zhang L, Jiang S, Wang X, Ding J, Zhang K. Decreased interhemispheric homotopic connectivity in Parkinson's disease patients with freezing of gait: a resting state fMRI study. *Parkinsonism Relat Disord* 2018; 52: 30–36
57. Zheng Z, Shemmassian S, Wijekoon C, Kim W, Bookheimer SY, Pouratian N. DTI correlates of distinct cognitive impairments in

- Parkinson's disease. *Hum Brain Mapp* 2014; 35(4): 1325–1333
58. Gorges M, Müller HP, Liepelt-Scarfone I, Storch A, Dodel R; LANDSCAPE Consortium, Hilker-Roggendorf R, Berg D, Kunz MS, Kalbe E, Baudrexel S, Kassubek J, Kassubek J. Structural brain signature of cognitive decline in Parkinson's disease: DTI-based evidence from the LANDSCAPE study. *Ther Adv Neurol Disorder* 2019; 12: 1756286419843447
  59. Vasconcellos LF, Pereira JS, Adachi M, Greca D, Cruz M, Malak AL, Charchat-Fichman H. Volumetric brain analysis as a predictor of a worse cognitive outcome in Parkinson's disease. *J Psychiatr Res* 2018; 102: 254–260
  60. Chan LL, Ng KM, Rumpel H, Fook-Chong S, Li HH, Tan EK. Transcallosal diffusion tensor abnormalities in predominant gait disorder parkinsonism. *Parkinsonism Relat Disord* 2014; 20(1): 53–59
  61. Galantucci S, Agosta F, Stankovic I, Petrovic I, Stojkovic T, Kostic V, Filippi M. Corpus callosum damage and motor function in Parkinson's disease (P2.006). *Neurology* 2014; 82(10 Supplement): P2.006
  62. Catani M, Jones DK, Donato R, Ffytche DH. Occipito-temporal connections in the human brain. *Brain* 2003; 126(9): 2093–2107
  63. Fox CJ, Iaria G, Barton JJ. Disconnection in prosopagnosia and face processing. *Cortex* 2008; 44(8): 996–1009
  64. Ffytche DH. The hodology of hallucinations. *Cortex* 2008; 44(8): 1067–1083
  65. Ross ED. Sensory-specific amnesia and hypoemotionality in humans and monkeys: gateway for developing a hodology of memory. *Cortex* 2008; 44(8): 1010–1022
  66. Catani M. From hodology to function. *Brain* 2007; 130(3): 602–605
  67. Catani M, Mesulam M. The arcuate fasciculus and the disconnection theme in language and aphasia: history and current state. *Cortex* 2008; 44(8): 953–961
  68. Rudrauf D, Mehta S, Grabowski TJ. Disconnection's renaissance takes shape: formal incorporation in group-level lesion studies. *Cortex* 2008; 44(8): 1084–1096
  69. Haghshomar M, Dolatshahi M, Ghazi Sherbaf F, Sanjari Moghadam H, Shirin Shandiz M, Aarabi MH. Disruption of inferior longitudinal fasciculus microstructure in Parkinson's disease: a systematic review of diffusion tensor imaging studies. *Front Neurol* 2018; 9: 598
  70. Lee E, Lee JE, Yoo K, Hong JY, Oh J, Sunwoo MK, Kim JS, Jeong Y, Lee PH, Sohn YH, Kang SY. Neural correlates of progressive reduction of bradykinesia in *de novo* Parkinson's disease. *Parkinsonism Relat Disord* 2014; 20(12): 1376–1381
  71. Wang M, Jiang S, Yuan Y, Zhang L, Ding J, Wang J, Zhang J, Zhang K, Wang J. Alterations of functional and structural connectivity of freezing of gait in Parkinson's disease. *J Neurol* 2016; 263(8): 1583–1592
  72. Tan SYZ, Keong NCH, Selvan RMP, Li H, Ooi LQR, Tan EK, Chan LL. Periventricular white matter abnormalities on diffusion tensor imaging of postural instability gait disorder parkinsonism. *AJNR Am J Neuroradiol* 2019; 40(4): 609–613
  73. Wu JY, Zhang Y, Wu WB, Hu G, Xu Y. Impaired long contact white matter fibers integrity is related to depression in Parkinson's disease. *CNS Neurosci Ther* 2018; 24(2): 108–114
  74. Duncan GW, Firbank MJ, Yarnall AJ, Khoo TK, Brooks DJ, Barker RA, Burn DJ, O'Brien JT. Gray and white matter imaging: a biomarker for cognitive impairment in early Parkinson's disease? *Mov Disord* 2016; 31(1): 103–110
  75. Reijnders JS, Ehrt U, Weber WE, Aarsland D, Leentjens AF. A systematic review of prevalence studies of depression in Parkinson's disease. *Mov Disord* 2008; 23(2): 183–189, quiz 313
  76. Yu J, Lam CLM, Lee TMC. White matter microstructural abnormalities in amnesic mild cognitive impairment: a meta-analysis of whole-brain and ROI-based studies. *Neurosci Biobehav Rev* 2017; 83: 405–416
  77. Bromis K, Calem M, Reinders AATS, Williams SCR, Kempton MJ. Meta-analysis of 89 structural MRI studies in posttraumatic stress disorder and comparison with major depressive disorder. *Am J Psychiatry* 2018; 175(10): 989–998
  78. Hawkes CH, Del Tredici K, Braak H. Parkinson's disease: a dual-hit hypothesis. *Neuropathol Appl Neurobiol* 2007; 33(6): 599–614
  79. Nigro S, Riccelli R, Passamonti L, Arabia G, Morelli M, Nisticò R, Novellino F, Salsone M, Barbagallo G, Quattrone A. Characterizing structural neural networks in *de novo* Parkinson disease patients using diffusion tensor imaging. *Hum Brain Mapp* 2016; 37(12): 4500–4510
  80. Zatorre RJ, Jones-Gotman M. Human olfactory discrimination after unilateral frontal or temporal lobectomy. *Brain* 1991; 114(Pt 1A): 71–84
  81. Doty RL. Olfactory dysfunction in Parkinson disease. *Nat Rev Neurol* 2012; 8(6): 329–339
  82. Berman BD, Smucny J, Wylie KP, Shelton E, Kronberg E, Leehey M, Tregellas JR. Levodopa modulates small-world architecture of functional brain networks in Parkinson's disease. *Mov Disord* 2016; 31(11): 1676–1684
  83. Dean DC 3rd, Sojkova J, Hurley S, Keckskemeti S, Okonkwo O, Bendlin BB, Theisen F, Johnson SC, Alexander AL, Gallagher CL. Alterations of myelin content in Parkinson's disease: a cross-sectional neuroimaging study. *PLoS One* 2016; 11(10): e0163774
  84. Degirmenci B, Yaman M, Haktanir A, Albayrak R, Acar M, Caliskan G. The effects of levodopa use on diffusion coefficients in various brain regions in Parkinson's disease. *Neurosci Lett* 2007; 416(3): 294–298
  85. Smith SM, Jenkinson M, Johansen-Berg H, Rueckert D, Nichols TE, Mackay CE, Watkins KE, Ciccarelli O, Cader MZ, Matthews PM, Behrens TE. Tract-based spatial statistics: voxelwise analysis of multi-subject diffusion data. *Neuroimage* 2006; 31(4): 1487–1505
  86. Zalesky A. Moderating registration misalignment in voxelwise comparisons of DTI data: a performance evaluation of skeleton projection. *Magn Reson Imaging* 2011; 29(1): 111–125
  87. Nortje G, Stein DJ, Radua J, Mataix-Cols D, Horn N. Systematic review and voxel-based meta-analysis of diffusion tensor imaging studies in bipolar disorder. *J Affect Disord* 2013; 150(2): 192–200